

The Impact of Visual Appearance on User Response in Online Display Advertising

Javad Azimi
azimi@eecs.oregonstate.edu
Oregon State University

Vidhya Navalpakkam
nvidhya@yahoo-inc.com
Yahoo! Labs, Silicon Valley

Ruofei Zhang
rzhang@yahoo-inc.com
Yahoo! Labs, Silicon Valley

Jianchang Mao
jmiao@yahoo-inc.com
Yahoo! Labs, Silicon Valley

Yang Zhou
yangzhou@yahoo-inc.com
Yahoo! Labs, Silicon Valley

Xiaoli Fern
xfern@eecs.oregonstate.edu
Oregon State University

November 27, 2024

Abstract

Display advertising has been a significant source of revenue for publishers and ad networks in online advertising ecosystem. One of the main goals in display advertising is to maximize user response rate for advertising campaigns, such as click through rates (CTR) or conversion rates. Although in the online advertising industry we believe that the visual appearance of ads (creatives) matters for propensity of user response, there is no published work so far to address this topic via a systematic data-driven approach. In this paper we quantitatively study the relationship between the visual appearance and performance of creatives using large scale data in the world's largest display ads exchange system, RightMedia. We designed a set of 43 visual features, some of which are novel and some are inspired by related work. We extracted these features from real creatives served on RightMedia. We also designed and conducted a series of experiments to evaluate the effectiveness of visual features for CTR prediction, ranking and performance classification. Based on the evaluation results, we selected a subset of features that have the most important impact on CTR. We believe that the findings presented in this paper will be very useful for the online advertising industry in designing high-performance creatives. It also provides the research community with the first ever data set, initial insights into visual appearance's effect on user response propensity, and evaluation benchmarks for further study.

1 Introduction

The Internet revolution has transformed how people experience information, media and advertising. Web advertising, although nonexistent twenty years ago, has become a vital component of the modern Internet, where advertisements are delivered from advertisers to users through different online channels. Recent trends have shown that an increasingly large share of advertisers' budgets are devoted to the online world, and online advertising spending has greatly outpaced some of the traditional advertising media, such as radio and magazine. Display advertising is one type of online advertising which, together with search advertising, contributes the majority of the revenue for many large Internet companies. In display advertising, display ad instances are shown to the user on webpages in different formats such as image, flash, and video. Each display ad instance is called a creative. By showing the creatives, advertisers aim to either promote brand awareness among users (brand advertising) or receive desirable responses from users (performance advertising), such as the action of purchasing, clicking or signing up for a promotion list from the advertiser's website. In performance advertising, the advertiser strives to optimize their ad's performance metrics such as the effective cost per click (eCPC) or effective cost per action (eCPA), which in turn relates to maximizing the user response rate on the creatives as measured by click through rates (CTR) or conversion rates (CVR). There are several factors that greatly influence the user response rate of display advertising campaigns: 1) the position of the ads on the webpage; 2) the relevancy of the ads to the online users, which is generally captured by the targeting profiles of the advertising campaigns; 3) the relevancy of the ads to the webpage content and 4) the quality and visual appearance of the creatives.

The problem of predicting the user response rate for online ads, especially CTR, has been studied by several researchers in the last few years. One major research focus has been in predicting clicks by studying the relationship between CTR and the aforementioned ad factors (and their combinations). For example in [2], the authors considered the ad's relevancy to the content of the webpage in predicting CTR. They show that improving the ad's content

relevancy is more efficient than considering the content of ads by themselves [25]. Although it is generally believed that visually appealing ads can perform better in attracting online users, as a result of which advertisers always care about the creative designs, there is no, to the best of our knowledge, published work so far to quantitatively study the effect of visual appearance of creatives on campaign performance in online display advertising. This motivates us to investigate the correlation between the visual features of the creative and CTR, regardless of other ad factors, and to predict creative performance based on its visual appearance alone.

Our proposed approach consists of two main steps, 1) feature extraction and 2) correlation investigation. We first extract some informative visual features from the creatives. We introduce 43 visual features classified into three categories, 1) *global features* which characterize the overall properties of a given creative, 2) *local features* representing the properties of specific parts within a given creative and 3) *advanced features* which are a group of features developed based on more complicated algorithms such as the number of faces and number of characters in a creative. We then develop three regression approaches to predict the CTR based on these features. The study is conducted using real creatives and their performance data from the world’s largest display ads exchange system, RightMedia. Based on the weights of developed features, we further select a subset of features that have high impact on the creative’s CTR. The benefit of this work is three-fold. First, our findings on the visual features and their relationship to CTR can provide useful recommendations to designers on what features to consider while designing creatives, and/or can help in automated creative generation. Second, the visual features and the regression methods developed here can be used in addition to the traditionally investigated ad factors (such as ad relevancy, position etc.) for improving CTR prediction in online ads selection. Third, it provides the research community with the first ever data set, initial insights into the effect of visual appearance on user response propensity, and evaluation benchmarks for further study.

The paper is organized as follows. Section 2 introduces the related work. We introduce the visual features in Section 3. The regression and feature selection results for CTR prediction are presented in Section 4, followed by our conclusion in Section 5.

2 Background and Related Work

The relationship between various print ad characteristics and measures of advertising effectiveness has been studied by advertising researchers for almost a century. A wide variety of characteristics have been investigated. These characteristics are roughly in two categories: mechanical and content-based. The mechanical characteristics include ad size, number of colors, proportional of illustrations to copy, the absence of borders, and type size. The content factors include message appeal like status, quality, fear and fantasy, attention-getting techniques like free offers, presence of women, and psycholinguistic variables like product or personal reference in headline, interrogative or imperative headline, visual rhetorics, among others. See [20] for summaries.

Even though the online advertising has taken a large market share of the advertising industry, and the whole industry is steadily and continuously shifting to the online domain, study on the effectiveness of the counterpart of print ads online, generally called display ads, is limited. We list the studies of several factors below.

Some existing studies try to investigate the effect of several different factors on the performance of display advertising campaigns. These factors include targeting and obtrusiveness [9], advertisement size (large vs. small) and ad exposure format (intrusive vs. voluntary) [4], cognitive impact from ad size and animation [18], emotional appeal and incentive offering in the ads [8], repetition of varied execution vs. single execution [30].

To the best of our knowledge, we are not aware of any study on the relationship between the visual appearance and the performance of creatives in online display ads. We try to tackle this problem by first defining a set of visual features and then evaluating their effects on ad performance, specifically CTR in our experiments, from the actively served ad campaigns on the world’s largest ad exchange system, RightMedia. Below, we present some previous computational studies on image properties which provide us inspiration in designing our visual features.

There are several studies that try to investigate a specific property of images (photos or paintings) using computational approaches. Such properties include quality and aesthetic in photos [19, 15, 29, 7] or in paintings [17], saliency [14], composition [10, 24], color harmony [5] and memorability [13].

Initial work on image quality evaluation concentrated on evaluating and reconstructing low graded, compressed or degraded images by simple noise model [6, 1]. However, in most of the beauty evaluation work, including this paper, we assume that high quality images are available and we are interested in evaluating the visual aesthetic of images based on visual features.

Recently some researchers tried to evaluate the beauty of an image based on its visual features. In [15] the authors aim to classify the pictures into professional and snapshot photos using some basic features including spatial distribution of edges, color distribution and hue count, etc. In [7] the authors introduced a regression based approach for

rating photos based on their beauty, using features such as average pixel density, colorfulness, saturation hue, and the rule of thirds. In addition to these studies, in [19] the author proposed an approach to classifying images into high and low quality. The main idea comes from the fact that a professional photographer makes the background blurry and the subject distinguishable in the image. By separating the blurry part of the image from the subject, they design a set of well-motivated features from both the subject and the whole image such as the clarity contrast of the subject, lighting, simplicity, color harmony and composition geometry. They show that the combination of these features can provide a promising performance. All of the above work tries to extract visual features from photos. Recently Li et al. [17] tried to extract some features from paintings to evaluate their beauty and classify them into high and low quality. They introduced a set of global and local features, 40 in total, to capture the painting properties such as the brightness contrast between segments, the brightness contrast across the whole image and the average saturation for the largest segment of the image.

Computational approaches have also been used to investigate other visual properties of an image. In [13] the authors studied what properties of images make them more memorable. They found that statistical properties of an image such as mean hue, mean saturation, intensity mean, intensity variance, intensity skewness and number of objects do not have any non-trivial correlation with memorability in their generated data set. However, they found that if they label the objects and scenes in the images, they can find a non-trivial and interesting correlation between images and their memorability. For example, their results show that the attendance of human being, close up objects and human scale objects in an image improve its memorability more than natural scene. This result is not possible to be applied to our work since it requires large amounts of supervision to tag different parts of the images. However, we evaluate the impact of the number of human faces in an image in our work.

Color harmonization is another approach for making an image more appealing. In [5] the authors proposed to harmonize the colors in a given image using harmonization templates from [31, 28], which include 8 different harmonized color templates. We also used color harmony models to evaluate the hue distribution of an image in our experiments.

In summary, existing work in related areas has focused primarily on properties of an image, photo or painting. In contrast, we examine creatives in online display ads, which contain both graphical features and text. In addition, some of the existing approaches require significant amount of supervision in their feature extraction step, which is not possible in large scale applications where we need to learn from large data sets with minimum amount of supervision. Finally, we would also like to extract a set of features that are visually understandable and can be practically controlled to guide the human designers or automatic creative generators (like in smart ads) to produce high-performance creatives. These objectives make our problem novel and interesting for the online advertising industry.

3 Feature Extraction

In this section we introduce a set of 43 different visual features. We categorize the developed features into three different sets, 1) global features, 2) local features and 3) advanced features. A complete list of the features can be found in Table 3. Below we describe the detailed definition of the proposed features in each category.

In the following sections we use I to indicate an image and use $|I|$ to indicate the size of the image measured by the number of pixels. We use variable x to denote an arbitrary pixel when we do not care about its location in the image. Otherwise we use (i, j) to denote the pixel in the i -th row and j -th column in the image.

3.1 Global Features

Global features are a set of features which represent the overall properties of the whole image. We describe the details of 19 different global features in this section.

3.1.1 Gray Level Features

We describe 3 features extracted from the gray level histogram of the image, namely the gray level contrast f_1 , number of dominant gray level bins f_2 , and the standard deviation of the gray level values among all pixels f_3 .

The gray level contrast is the width of the middle 95% mass in the gray level histogram [15]. From the original gray level histogram, we prune the extreme 2.5% from the 0 side and 2.5% from the 255 side. Gray level contrast feature f_1 is calculated as the width of the remaining histogram.

We count the number of dominant bins in the gray level histogram as our second feature. Suppose the set $G = \{g_0, g_1, \dots, g_{255}\}$ indicates the set of 256 bins in the gray level histogram such that g_i is the number of pixel in i -th

bins. We define the number of dominant gray level bins as $f_2 = \sum_{k=0}^{255} \mathbf{1}(g_k \geq c_1 \max_i g_i)$, where $\mathbf{1}(\cdot)$ is the indicator function and c_1 is a threshold value which is set to be 0.01 in this paper.¹

The last gray level feature, f_3 , is defined as the standard deviation of gray level values of all pixels in the image. It is used to capture the variance of the gray level distribution.

3.1.2 Color Distribution

To avoid distraction from objects in the background, professional photographers tend to keep the background simple. In [19], the authors use the color distribution of the background to measure this simplicity. We use a similar approach to measure the simplicity of color distribution in the image. For a given image, we quantize each RGB channel into 8 values, creating a histogram $H_{rgb} = \{h_0, h_1, \dots, h_{511}\}$ of 512 bins, where h_i indicates the number of pixels in i -th bin. We define feature f_4 to indicate the number of dominant colors as $f_4 = \sum_{k=0}^{511} \mathbf{1}(h_k \geq c_2 \max_i h_i)$ where $c_2 = 0.01$ is the threshold parameter. We also calculate the size of the dominant bin relative to the image size as $f_5 = \frac{\max_i h_i}{|I|}$. This feature indicates the extent to which one of 512 colors is dominant in the image.

By replacing the RGB color map with HSV (Hue, Saturation, Value) color map and using the above methods in calculating features f_4 and f_5 , we obtain two other features f_6 and f_7 .

3.1.3 Model-Based Color Harmony

The concept of color harmony in this paper is based on 8 different harmonic color distributions (illustrated in Figure 1) that are based on the hue of the HSV color wheel [31]. These distributions are called i, V, L, I, T, Y, X, N . Note that each distribution can be rotated by $0 \leq \alpha \leq 360$ degrees. The specific size of color harmony distributions are set as follows: the large sectors of types V, Y and X are 26% of the disk (93.6°); the small sectors of types i, L, I and Y are 5% of the disk (18°); the largest sector of type L is 22% of the disk (79.2°); the sector of type T is 50% of the disk (180°). The angle between the centers of the two sectors is 180° for I, X, Y , and 90° for L .

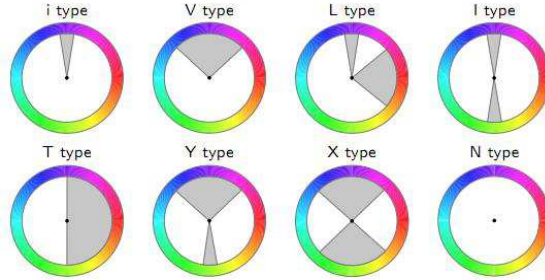


Figure 1: Color harmony models

Let us define the set of 8 distributions as $\mathcal{D} = \{d^1, d^2, \dots, d^8\}$. We say $\phi(d_\alpha^i, x)$ indicates the hue of the closest point in the i -th distribution to x after α degree rotation, where x is any arbitrary pixel in the image. We compute the distance between the hue distribution of our image I and the distribution $d^i \in \mathcal{D}$ as:

$$\gamma(I, d^i) = \argmin_{\alpha} \frac{1}{|I|} \sum_{x \in I} \| \text{hue}(x) - \phi(d_\alpha^i, x) \| \cdot \text{sat}(x), \quad (1)$$

where $\text{hue}(x)$ and $\text{sat}(x)$ indicate the hue and saturation at pixel x , and $\| \cdot \|$ denotes the arc-length distance. We are interested in the best fitting model d^* which has the least $\gamma(\cdot)$ value, $d^* = \argmin_{d^i} \gamma(I, d^i)$. We define feature $f_8 = \gamma(I, d^*)$. Intuitively, it tells us how different is the hue distribution of image I from the best fitting model of color harmony.

Some models are superset of other models in Figure 1 concluding that the $\gamma(\cdot)$ value of some smaller models are higher than some larger models given any image I , e.g. $\gamma(I, d_i) \geq \gamma(I, d_V) \geq \gamma(I, d_T)$. Therefore, if an image hue distribution fits into some small models, type i, V, L, I , it fits into larger models as well. This can emphasize the color harmony property of the images which can fit into a few models rather than just one model. We consider this property as one potential positive property of the image. To quantify this property, we introduce a new feature, f_9 , which indicates the average color harmony deviation from the best two fitted models given an image I . In general, in

¹This parameter, and similar ones in the rest of the paper, is set inspired by related works such as [19].

addition to the deviation from the best fitted model illustrated by feature f_8 , we consider the deviation from the second best fitted model as well, and the average of these two deviations is returned as f_9 . Clearly, for the images fitting into small color harmony models, we will have f_8 and f_9 very close to each other. However, for the images which fit into the largest model, we will have f_9 considerably larger than f_8 . We believe these two numerical features can represent the color harmony property of an image appropriately.

3.1.4 Color Coherence

We extract a set of features based on the color coherence of pixels resulting in connected coherent components [23]. A connected coherent component in an image is defined as:

- A set of pixels that fall into the same bin in the histogram.
- For any two pixels p_i and p_j in a connected coherent component $P = \{p_1, p_2, \dots, p_m\}$ of m pixels, there is a path of sequential pixels, p_i, p_{i+1}, \dots, p_j . Two sequential pixels in a path must be one of the 8 neighborhoods of each other.
- The size of the connected coherent component is larger than a predefined threshold c_4 . In our experiment we set $c_4 = 0.01|I|$.

We denote the set of connected coherent components and their color index as $\mathcal{P} = \{(P_1, h_1), (P_2, h_2), \dots, (P_n, h_n)\}$, where P_i is the set of pixels in the i -th component, and h_i is its corresponding color in the HSV color histogram with 512 bins. We use $|P_i|$ to denote the number of pixels in P_i . We extract the following features based on the above definition:

- $f_{10} = n$, which indicates the number of connected coherent components in the image.
- $f_{11} = \frac{\max_i |P_i|}{|I|}$, which indicates the size of the largest component relative to the whole image.
- $f_{12} = \frac{\max_{j, j \neq \arg \max_i |P_i|} |P_j|}{|I|}$, representing the size of the second largest connected coherent component relative to the whole image.
- $f_{13} = \text{rank}(h_i), i = \arg \max_j |P_j|$, indicating the rank of the bin, considering the bin size in descending order, associated with the largest connected coherent component in the image. For example, the value of this feature is 1 if the bin associated with the largest coherent component, $\arg \max_j |P_j|$, is the largest bin in the color histogram as well; $\max_i |h_i|$ where h_i is the size of the i -th bin in the color histogram. This feature indicates how the colors are disperse in the image. We expect to have value $f_{13} = 1$ if the colors in the images are not very randomly distributed. It means the pixel with the same colors are mostly connected together.
- $f_{14} = \text{rank}(h_i), i = \arg \max_{j, j \neq \arg \max_k |P_k|} |P_j|$, similar to f_{13} , it shows the bin rank, considering the bin size in descending order, of the second largest connected coherent component in the image.

3.1.5 Hue Distribution

In this section we introduce three features based on the hue in HSV color space. We quantize hues in an image in a similar way as in [17] by eliminating the pixels with saturation and value less than 0.2. This will eliminate all the pixels with white or black colors. Then we calculate the hue histogram of remaining pixels with 20 different bins, 18° for each bin, which results in $\mathcal{H}_{hue} = \{h_1, h_2, \dots, h_{20}\}$ where h_i indicates the set of pixels in i -th bin. We then extract the following features:

- $f_{15} = \sum_{i=1}^{20} \mathbf{1}(|h_i| \geq c_5|I|)$ where $c_5 = 0.01$ in our experiments. This feature indicates the number of dominant hues in an image.
- $f_{16} = \max_{i,j} \| |h_i| - |h_j| \|$ where $|h_i| \geq c_5|I|$, and $\| \cdot \|$ is the arc length. This feature indicates the largest contrast between two dominant hues in the image.
- $f_{17} = \text{std}(\Phi)$ where $\Phi = \{\cup_{i \in I} \| h_i(i) - 0 \| \}$ and $\| \cdot \|$ is the arc length value. This feature indicates the standard deviation of all pixel's hues distance from the origin 0. It simply can determine how much the hue colors in an images has been distributed from each other.

3.1.6 Lightness Features

We use the lightness L in the HSL color space to calculate feature f_{18} and f_{19} . In the HSL color space, L value is small when the color is white and is large when the color is black. The L value in HSL color space can be calculated as follows:

$$L(x) = \frac{\max(r(x), g(x), b(x)) + \min(r(x), g(x), b(x))}{2}, \quad (2)$$

where $r(x), g(x), b(x)$ denotes the R, G, B values of pixel x in RGB color space. We calculate two lightness features as:

- $f_{18} = \frac{1}{|I|} \sum_{x \in I} L(x)$, the average lightness of pixels in the image.
- $f_{19} = \text{std}(L(\cdot))$, the standard deviation of lightness of all pixels in the image.

3.2 Local Features

Local features represent a set of features extracted from specific parts of the image rather than the whole image. We apply the normalized cut segmentation method [26] to partition the image into 5 smaller segments. Let $S = \{S_1, S_2, \dots, S_5\}$ indicate the set of 5 different segments where S_i is the set of pixels in segment i . Note that a segment is considered as noise and is dropped if it is smaller than 5% of the image. We develop the following features based on the segmentation result.

3.2.1 Segment Size

Two features are extracted from segment size as follows:

- $f_{20} = \frac{\max_i |S_i|}{|I|}$, indicating the size of the largest segment relative to the whole image.
- $f_{21} = \frac{1}{|I|} \max_{i,j} ||S_i| - |S_j||$, indicating the contrast among the segmentation sizes of the image.

3.2.2 Segment Hues

Similar to section 3.1.5, we generate the hue histogram of each segment. We define the set of hue histograms of all 5 segments as $\mathcal{H}_{hue}^s = \{h_{1,1}, h_{1,2}, \dots, h_{1,20}, h_{2,1}, \dots, h_{5,20}\}$ where $h_{i,j}$ indicates the set of pixels that fall in the j -th bin of i -th segment. Then we extract five features to capture different hue properties. Below we describe the formal definition of developed features:

- $f_{22} = \sum_{j=1}^{20} \mathbf{1}(|h_{i,j}| \geq c_6 |I|)$ where $i = \arg \max_i |S_i|$ and $c_6 = 0.01$. This feature denotes the number of image-wide dominant hues in the largest segment. In general, we would like to have most of the image hues in the largest segment.
- $f_{23} = \sum_{j=1}^{20} \mathbf{1}(|h_{i,j}| \geq c_6 |S_i|)$ where $i = \arg \max_i |S_i|$. This feature denotes the number of segment-wide dominant hues in the largest segment.
- $f_{24} = \max_i q_i$ where $q_i = \sum_{j=1}^{20} \mathbf{1}(|h_{i,j}| \geq c_6 |S_i|)$ is the number of dominant hues in i -th segment. This feature essentially denotes the largest number of dominant hues in one segment. We would like to have the same value as f_{23} for this feature illustrating that the largest segment has the largest number of dominant colors.
- $f_{25} = \max_{i,j} |q_i - q_j|$. This feature denotes the contrast of the number of dominant hues among the segments. We usually do not like to have lots of different hues in one segment and a few hues in another segment in an image. We expect to have unappealing images with large value for f_{25} .
- $f_{26} = \max_{j,k} ||h_{i,j} - h_{i,k}||$ where $|h_{i,j}|, |h_{i,k}| \geq c_6 |S_i|$, $i = \arg \max_i |S_i|$ and $||\cdot||$ is the arc length distance. This feature captures the contrast of number of pixels among the hue bins in the largest segment. In general, we expect to have an appealing image with one bin dominating the largest segment in addition to a few more small bins. This makes the contrast value very large.
- $f_{27} = \text{std}(T(\cdot))$ where $T(i) = \max_{j,k} |h_{i,j}|, |h_{i,k}| \geq c_6 |S_i|$. This feature returns the standard deviation of contrast among the segments. If we have different hue contrasts among different segments, this feature will achieve a significant value.



Figure 2: The saliency map of an image. Left: original image. Right: saliency map.

3.2.3 Segment Color Harmony

Two features are extracted based on the largest segment color harmony. Feature f_{28} is the minimum deviation from the best fitted color harmony model for the largest segment, and feature f_{29} is the average deviation of the best two fitted color harmony models for the largest segment. The details of color harmony models have been introduced in section 3.1.3.

3.2.4 Segment Lightness

Three segment lightness features are extracted using similar method as in section 3.1.6:

- f_{30} : average lightness in the largest segment.
- f_{31} : standard deviation of average lightness among the segments.
- f_{32} : contrast of average lightness among the segments.

3.3 Advanced features

In this section we develop a set of features based on more complicated algorithms. Most of the advanced features are based on the saliency map of the image which determines the visually salient areas in the image that are more likely to be noticed by the humans. We also extract two additional features related to the number of characters and number of faces in an image. Below we describe the details of these features.

3.3.1 Saliency Features

Saliency computation is a well known phenomenon in human vision where attention tends to be drawn to interesting parts of an image that appear visually different from the rest of the image (e.g., a red coke can in a green background appears salient and is immediately noticed, while the same coke can in an orange-reddish background is not salient and less likely to be noticed). We compute saliency according to the algorithm described in [12]. Figure 2 shows the saliency output of the algorithm presented in [12] for a sample creative. The areas with higher lightness in the saliency map indicate more salient part of the image.

The saliency algorithm returns a matrix τ (also referred to as saliency map) where $\tau(i, j)$ represents the saliency value of pixel (i, j) . We also extract a binary image based on the saliency map, by setting a threshold α to the saliency map where the pixels with saliency value larger than α are set to 1 and the rest of the pixels are set to 0. Similar to [12], the parameter α is set as $\alpha = 3\bar{\tau}$ where $\bar{\tau} = 1/n \sum_{i,j} \tau(i, j)$ is the average saliency value in the image. After this binarization, we have some connected components with value 1. These components indicate saliency areas, and the other parts of the image are considered as background. Then we extract the following features based on the saliency results, saliency map and binary saliency map.

- f_{33} : background size. Salient objects usually appear in the foreground and not in the background. Therefore we return the size of the background as a function of image size which is calculated as: $f_{33} = \frac{\sum_{i,j} \mathbf{1}(\tau(i,j) < \alpha)}{|I|}$.
- f_{34} : number of connected components in the binary map.
- f_{35} : size of the largest components in the binary saliency map relative to the whole image.



Figure 3: The four interested points based on rule of third.

- f_{36} : average saliency value of the largest component in the binary saliency map.
- f_{37} : number of connected components in the image background. In some images, the saliency areas can divide the background into several disconnected segments. Usually it is not desirable to have multiple background components.
- f_{38} : size of the largest connected component in the background relative to the whole image. If the number of connected components in the background is equal to one, then this feature has the same value as f_{33} .
- f_{39} : distance between connected components. Let the set $\mathcal{C} = \{c_1, c_2, \dots, c_n\}$, $c_i = (x_i, y_i)$ indicates the set of n different points such that each c_i indicates a pixel corresponding to the center of mass of the i -th saliency area. To make the rest of the computation scale independent from the image size, we update the properties of each point c_i as $s_i = (x_i/I_x, y_i/I_y)$ such that I_x and I_y are the horizontal and vertical size of the image. Then we build up a complete weighted graph given the set \mathcal{C} such that the weight $w_{i,j}$ between two vertices c_i, c_j is calculated as $w_{i,j} = \|s_i - s_j\|_2$. Then we return the summation of all edge weights as the distance between connected components.
- f_{40} : distance from the rule of third points. Professional photographers usually locate their main object in one of the four interest points based on the rule of third. The four interest points in rule of third is the intersection of two vertical and two horizontal lines dividing the image into 9 equal segments. Figure 3 shows the four interested points based on rule of third. This is an important feature in photo beauty evaluation [17], motivating us to investigate its effect in creative performance. We define this feature as the minimum distance from the center of mass of the largest saliency area to one of the four interest points based on rule of third.
- f_{41} : distance from the center of image. This feature is the distance of saliency components to the center of image which is the most focused part of an image. The overall distance from the centers of all connected components to the center of image is returned as feature f_{41} . Note that for both features f_{40} and f_{41} , we normalize the position of each pixel similar as feature f_{39} .

3.3.2 Number of Characters

We consider the number of characters in an image as feature f_{42} . We tried a number of OCR toolbox and one of them provides us with appropriate results considering the number of characters in ads[22]. Note that we are interested in the number of characters in the image regardless of its meaning. To evaluate the accuracy of the OCR toolbox, we counted the true number of characters in 100 random images and compared it to the returned number of characters from the OCR toolbox. We found strong linear correlation of 0.80, suggesting that our toolbox is reasonably accurate in evaluating the number of characters in images. Note that extracting the exact text from ad creatives is challenging as they often appear in different fonts, sizes and orientations.

3.3.3 Number of Faces

The last feature, f_{43} , captures the effect of the human face appearance on creative performance. In [13] the authors concluded that the human appearance in an image could make the image more memorable. This motivates us to test whether face appearance affects creative performance. We count the number of faces in an image using an available toolbox [16]. Our toolbox is reasonably accurate and has a correlation more than 0.9 with the true number of faces in images in our experiments with a sample size of 100.

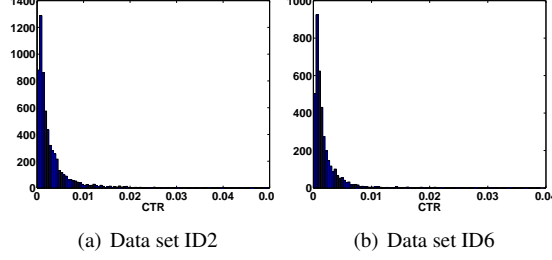


Figure 4: The CTR distribution of two data sets.

4 Experimental Results

In this section we present the algorithms and experiments we designed to evaluate the relationship between visual features and the performance of creatives in online display advertising.

4.1 Data Set

We extracted creatives of advertising campaigns from the world’s largest online advertising exchange system, Right-Media. We filtered out animated creatives because our features are designed for static images. We also calculated the average CTR of these creatives from online serving history log during a two-month period.

As discussed in Section 1, the performance of creatives is determined by many factors. One important factor is the ad position in the webpage. Generally the available position of a creative on a webpage is determined by the creative’s size. To remove the impact on performance introduced by ad position (and size), we create two different data sets, each of which consists of creatives with the same size. The first data set, ID2, consists of 6272 creatives with size 250×300 pixels, and the second data set, ID6, includes 3888 images with 90×730 pixels. All of the creatives have a minimum of 100K impressions guaranteeing that their CTRs have converged to their true values. The CTR distribution of each data set is shown in Figure 4.

We further created two sub-categories from data set ID2: “dating” with 927 images and “traveling” with 599 images. Since there are not many images in these two categories, we consider the images with a minimum of 20k and 10k impressions for “dating” and “traveling” respectively.

4.2 Learning Methods

The main goal of this work is to study the relationship between the performance of creatives and their visual features. In the first step we try to predict CTR from visual features using regression methods. We used three different regression algorithms to predict CTR, 1) Linear Regression (LR), 2) Support Vector Regression with RBF kernel(SVR), and 3) Constrained Lasso (C-Lasso) which is a modification to Lasso [27].

We used LIBSVM [3] to implement the SVR and performed cross validation to determine the parameters of the model. We describe our constrained Lasso optimization approach as follows. Suppose we have a set of n creatives at disposal and the visual features of these creatives are represented as a matrix $A \in \mathbf{R}^{d \times n}$ such that $A = (\mathbf{a}_1, \mathbf{a}_2, \dots, \mathbf{a}_n)$ where $\mathbf{a}_k \in \mathbf{R}^d$ is a column vector representing the d dimensional visual features of creative k . In our experiment $d = 43$. The CTR values of the n creatives are represented as a vector $\mathbf{y} = (y_1, \dots, y_n)^\top \in \mathbf{R}^n$ where each y_k is the CTR of the k -th creative. We bound the CTR of each creative by $y_{min} \leq y_i \leq y_{max}$ where y_{min} and y_{max} can be obtained from online serving history log. To predict CTR of the creatives, we try to solve the following optimization problem:

$$\begin{aligned} \min_w \quad & \|A^\top \mathbf{w} - \mathbf{y}\|_F^2 + \lambda \|\mathbf{w}\|_1 \\ \text{s.t.} \quad & y_{min} \leq A^\top \mathbf{w} \leq y_{max} \end{aligned} \quad (3)$$

where $\|\cdot\|_F^2$ is Frobinus-2 norm and $\|\cdot\|_1$ is ℓ_1 norm, also called lasso. We call the above optimization problem as constrained Lasso (C-Lasso) and we used [11] to find the solution of this optimization problem. Note that the proposed C-Lasso approach performs better than Lasso in our application.

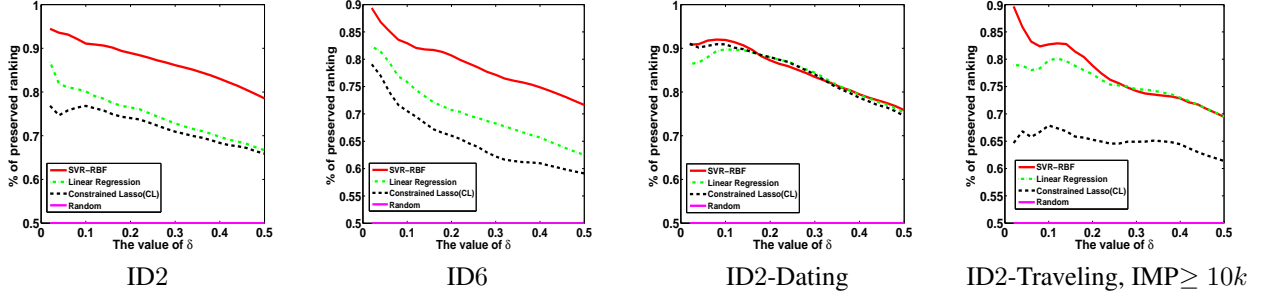


Figure 5: The amount of preserved ranking for each method.

Table 1: The prediction accuracy of each method against *Random* policy.

Data set	Samples	CM	LR	C-Lasso	SVR
ID2	6272	1.71	2.28	2.22	3.27
ID6	3888	1.75	2.27	2.14	2.77
ID2-Dating	927	1.79	2.65	2.58	2.79
ID2-Traveling	599	1.68	2.13	2.03	2.26

4.3 Evaluation

In this section we present different evaluation methods to analyze the efficacy of the developed visual features in predicting the performance of creatives.

4.3.1 CTR Prediction

To evaluate the CTR prediction accuracy of the algorithms, we run each algorithm for 200 independent runs where in each run 80% of each data set is selected randomly for training and 20% for testing. The accuracy evaluation results are reported over the prediction of the test data. Mean Squared Error (MSE) is used to measure the prediction accuracy for each algorithm as follows:

$$MSE = \frac{1}{n} \sum_{k=1}^n |y_k - \hat{y}_k|^2 \quad (4)$$

where n is the number of test samples, y_k is the true CTR of the k -th creative calculated from history log, and \hat{y}_k is the predicted CTR. To meaningfully interpret the MSE value, we introduce two baseline approaches, *Random* and *Constant Mean(CM)* policy.

The *Random* policy simply samples from the CTR distribution of the training data to predict the CTR of each testing creative, while the CM policy assigns a constant value, c_m , to all ads where c_m is the mean CTR of the training data. Table 1 shows the average results over 200 independent runs for each algorithm. Each entry is the MSE value of the random policy divided by MSE value of each algorithm. Results show that we can perform up to 3.27 times better than *Random* policy in predicting the CTR from visual features only. All learners perform consistently better than baseline CM as well. This result demonstrates the non-trivial impact of visual appearance of the creative on its advertising performance.

4.3.2 CTR Ranking

We introduce a ranking criterion to investigate the ability of using visual features to rank the creatives by their CTRs. Given a test set of creatives, suppose $c_1^-, c_2^-, \dots, c_k^-$ represent the k images with the lowest CTR values and $c_1^+, c_2^+, \dots, c_k^+$ represent the k images with the highest CTR. Therefore we have k^2 pairs (c_i^-, c_j^+) such that $ctr(c_i^-) \leq ctr(c_j^+)$ for $i, j \in \{1, \dots, k\}$. We wish to know whether our prediction of CTR using visual features preserves the ranking of pairs (c_i^-, c_j^+) . To test this, we change the value of k as a function of test data size. We then measure the percentage of match between the predicted ranking of creatives, and the truly observed ranking in the test data. The results over 200 independent runs are shown in figure 5 for different data sets. The x -axis indicates the

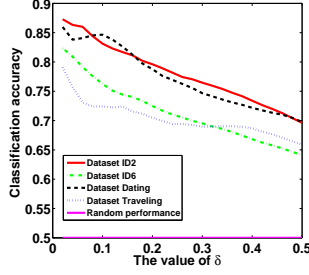


Figure 6: The classification accuracy for each data set.

value of δ such that $k = \delta n$ for $\delta = 0.02, 0.04, 0.06, \dots, 0.50$ where n is the number of creatives in the data set, and y -axis represents the percentage of correctly ranked pairs.

Results show that SVR consistently outperforms other learners. As we increase the size of k , the percentage of correctly ranked predictions decreases for all learning algorithms. This is as expected, since differentiating the images of creatives which have CTRs close to the mean of the CTR distribution, using visual features only, is very difficult even for a human. Interestingly, the results show that by just using visual features, we can preserve more than 90% of the ranking for data set ID2 (for $\delta = 0.1$). This number remains high at 75% when we consider all top-half images against low-half images for all data sets ($\delta = 0.5$). This is an encouraging result that demonstrates the utility of visual features in predicting the ranking of CTR.

4.3.3 CTR Classification

Previous studies in beauty evaluation [7, 15, 17] mostly try to classify the images into high and low quality category rather than assigning scores to their beauty based on visual features. Similarly, we evaluate the performance of classifying the creatives into high (+1) and low (-1) CTR category using visual features only. We use support vector machine with RBF kernel as our classifier. Similar to the previous section, we randomly separate 80% of data as training and use the rest as testing data. Then, we train our classifier on creatives that belong to the top and bottom 30% in CTR. In fact, we are disregarding 40% of data that are close to the training data CTR mean, μ_t , to reduce the noise for the classifier. Similar to the ranking experiments, we filter our test set by focusing on the k creatives with highest CTR values (labeled as positive) and the k creatives with the lowest CTR values (labeled as negative), where $k = \delta n$ is varied by changing δ . We obtain the classification accuracy by comparing the predicted classes to the true classes obtained from real CTR values. Figure 6 demonstrates the average classification accuracy over 200 independent runs where each run uses randomly selected training and testing data. The x -axis indicates the value of δ and y -axis represents the classification accuracy for each data set given a fixed value of δ . As seen in the figure, using visual features yields a classification accuracy of 70% when $\delta = 0.5$. Together with the previous results on predicting and ranking CTR, these results show the efficacy of using visual features of creatives in predicting CTR.

4.4 Feature Selection

The above analysis shows that visual features are useful in predicting the performance of creatives in online advertising. A natural question is to identify the visual features that have strong impact on ad performance. Such information could be very useful in many areas. For example, human graphic designers may use this information to guide their design of high-performance creatives. Smart ads system may use this information to dynamically generate creatives that are more appealing to online users. Ad exchange system may use this information to determine which creative will win in the auction marketplace for each advertising opportunity. In this section we conduct a series of experiments to select such important visual features.

We first calculate the Linear Correlation (LC) and Mutual Information (MI) between all features and CTR in each data set. Mutual information can provide us with the information of non-linear correlation between features. Note that, to calculate the mutual information between any pair of features (X, Y) , we discretized each feature and CTR values into 50 equal intervals. The results are shown in table 3. The top 5 features in each data set with highest absolute values are highlighted in bold. The table shows that there is no feature with high linear correlation or mutual information except f_{12} in data set ID6. Thus we use Forward Feature Selection (FFS) to select the top k features.

Before running FFS, we first cluster the features based on the Normalized Mutual Information (NMI) of all feature

Table 2: The top 10 selected clusters by FFS.

Data Set	Selected Clusters
ID2	$S_5, S_1, S_{19}, S_{17}, S_{13}, S_{18}, S_{20}, S_{10}, S_{11}, S_9$
ID6	$S_1, S_2, S_{20}, S_5, S_{17}, S_{14}, S_9, S_{13}, S_4, S_{18}$

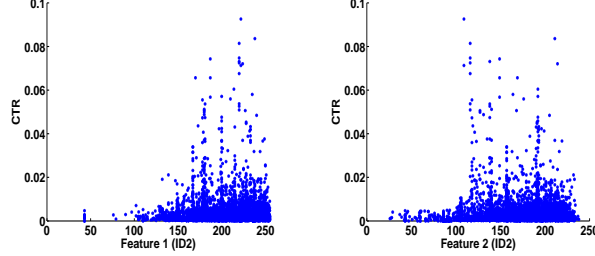


Figure 7: The scatter plot of f_1 and f_2 against CTR.

pairs. We discretize each feature into 50 equal intervals, and calculate NMI as follows:

$$NMI(X; Y) = \frac{I(X; Y)}{\sqrt{H(X)H(Y)}}, \quad (5)$$

where $H(X)$ is the entropy of random variable X . Then we cluster the features using the average linkage algorithm [21]. Two clusters are merged into one if their average NMI is at least 0.2. This results in 20 clusters for data set ID2 and 21 clusters for data set ID6. The resulting clusters are shown in Table 3. In the table, S_i represents a set of features in cluster i . We now apply a simple change to the FFS algorithm to select the top k clusters rather than features. After selecting a feature by FFS, all the correlated features that belong to the same cluster are removed from the next steps of FFS. The selected top $k = 10$ clusters are shown in table 2. Note that clustering the features in the above manner helps select different features (or feature sets) that are less correlated with each other. For example, all color harmony features are in the same cluster S_4 . Therefore by selecting one of the features from this cluster, we indicate the importance of color harmony in CTR, and by removing the highly correlated features at each step in FFS, we can guarantee to select a set of features which are less correlated with each other. Below we investigate some of the selected clusters that are common to both data sets.

Table 2 shows that S_1 is the best feature set (or cluster) for data set ID6 and the second best set for data set ID2 which illustrates the importance of set S_1 . S_1 consists of the gray level features f_1 and f_2 of the image. The scatter plot of both features in data set ID2 is shown in Figure 7 (the scatter plot in data set ID6 is similar). Figure 7 shows that for creatives with small value in both features, high CTR value is unlikely, and creatives with high CTR values should have high values in these two features. This is consistent with the intuition that creatives with higher contrast should perform better. Note that having high values in these two features does not guarantee a high CTR value.

S_5 is the best feature set for data set ID2 and the fourth for ID6. It only includes f_{10} which is the number of connected coherent components. The scatter plot of f_{10} in both data sets are shown in figure 8. The scatter plot shows that creatives with more than 15 connected coherent components in data set ID6 and more than 20 in data set ID2 are unlikely to achieve a CTR higher than 0.01. In other words, this suggests that cluttered creatives containing many objects tend to have lower CTR.

The number of characters, S_{19} in data set ID2 and S_{20} in data set ID6, is interestingly the third important feature set in both data sets. Figure 9 shows the scatter plot of the number of characters in both data sets. It can be seen that the creatives with higher number of characters are unlikely to achieve high CTR values in both data sets, once again suggesting that textual clutter is undesirable.

The next selected categories is S_{17} which is the 4-th selected category in ID2 and the 5-th in ID6. S_{17} represents the number of connected components in saliency binary map, distance between salient components, distance of saliency areas from the center of image and rule of third closest point. This indicates the importance of saliency features as well as considering professional photography rules such as the rule of third in designing ads. Intuitively, a small number of salient components, closer to the center of the creative, and consistent with the rule of third are desirable features in a creative. Finally, S_{13} , which contains features describing the number of hues and the contrast of hues in the largest

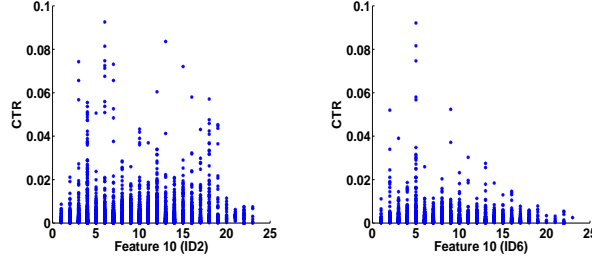


Figure 8: The scatter plot of f_{10} .

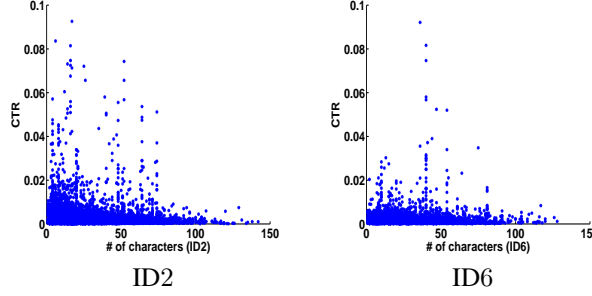


Figure 9: The scatter plot of number of characters.

segment of the image, is the 5-th important common category considering both data sets. Note that the scatter plot of the last 2 selected categories have been omitted due to space limit. In summary, our top 5 selected categories include the features from all proposed feature categories, global, local and advanced features, indicating the importance of each of them in predicting the creatives CTR.

5 Conclusion

In this paper we investigated the relationship between the user response rate and the visual appearance of creatives in online display advertising. To the best of our knowledge, this is the first work in this area. We designed 43 visual features for our experiments. We extracted the features from large scale data produced by the world’s largest ad exchange system. We tested the utility of visual features in CTR prediction, ranking and classification. The experimental results demonstrate that our proposed framework is able to outperform baseline consistently, indicating the efficacy of visual features in predicting CTR. We also performed feature selection to select the top visual feature categories that have strongest importance for increasing CTR. The findings from this work will be useful for ads selection and developing visually appealing creatives with higher user response propensity in online display advertising.

References

- [1] Bovik, A. C., Cormack, L. K., Aggarwal, J. K., Bajaj, C., Veciana, G. D., Ghosh, J., Sheikh, H. R., Sheikh, H. R., and Sc, B. (2005). No-reference quality assessment using natural scene statistics: Jpeg2000. *JPEG2000*.
- [2] Chakrabarti, D., Agarwal, D., and Josifovski, V. (2008). Contextual advertising by combining relevance with click feedback. In *WWW*, pages 417–426.
- [3] Chang, C.-C. and Lin, C.-J. (2011). LIBSVM: A library for support vector machines. *ACM Transactions on Intelligent Systems and Technology*.
- [4] Chatterjee, P. (2008). Are unclicke ads wasted? enduring effects of banner and pop-up ad exposures on brand memory and attitudes. *Journal of Electronic Commerce Research*, pages 51–61.

Table 3: Complete list of visual features.

Feature	Short Description	LC ID2	MI ID2	LC ID6	MI ID6	C-ID2	C-ID6
f_1	gray level contrast	-0.048	0.063	-0.102	0.098	S_1	S_1
f_2	number of dominant bins in gray level histogram	-0.107	0.071	-0.137	0.112	S_1	S_1
f_3	standard deviation of gray level images	-0.063	0.061	-0.016	0.082	S_2	S_2
f_4	number of dominant bins in RGB histogram	-0.083	0.067	-0.074	0.078	S_3	S_3
f_5	size of the dominant bin in RGB histogram	0.078	0.093	0.064	0.104	S_3	S_3
f_6	number of dominant bins in HSV histogram	-0.083	0.073	-0.078	0.092	S_3	S_3
f_7	size of the dominant bin in HSV histogram	0.119	0.096	0.085	0.094	S_3	S_3
f_8	deviation from the best color harmony model	-0.062	0.039	-0.040	0.052	S_4	S_4
f_9	average deviation from the best two color harmony models	-0.069	0.047	-0.046	0.063	S_4	S_4
f_{10}	number of connected coherent components	0.094	0.062	-0.004	0.064	S_5	S_5
f_{11}	size of the largest connected coherent component	0.102	0.090	0.069	0.099	S_3	S_3
f_{12}	size of the second largest connected coherent component	0.085	0.068	0.315	0.122	S_6	S_6
f_{13}	color size rank of the largest connected coherent component	-0.002	0.010	-0.012	0.014	S_7	S_7
f_{14}	color size rank of the second largest connected coherent component	-0.046	0.020	-0.039	0.022	S_8	S_8
f_{15}	number of dominant hues	-0.102	0.036	-0.119	0.045	S_9	S_9
f_{16}	contrast of dominant hues	-0.015	0.027	-0.015	0.046	S_9	S_9
f_{17}	standard deviation of hues	0.010	0.084	-0.039	0.102	S_{10}	S_{10}
f_{18}	average lightness	0.031	0.072	0.035	0.099	S_{11}	S_{11}
f_{19}	standard deviation of lightness	-0.065	0.063	-0.086	0.084	S_2	S_2
f_{20}	size of the Largest Segments (LS)	-0.052	0.058	-0.080	0.081	S_{12}	S_{12}
f_{21}	segments size contrast	-0.044	0.054	-0.122	0.092	S_{12}	S_{12}
f_{22}	number of image dominant hues in the LS	-0.104	0.044	-0.068	0.029	S_{13}	S_{13}
f_{23}	number of dominant hues in the LS	-0.102	0.032	-0.080	0.036	S_{13}	S_{13}
f_{24}	largest number of dominant hues in one segment	-0.079	0.031	-0.125	0.045	S_{14}	S_{14}
f_{25}	contrast of hues number among segments	-0.006	0.027	-0.098	0.033	S_{14}	S_{14}
f_{26}	contrast of hues in the LS	-0.120	0.032	-0.085	0.036	S_{13}	S_{13}
f_{27}	standard deviation of hues contrast among segments	-0.056	0.072	-0.073	0.098	S_{10}	S_{10}
f_{28}	deviation from the best color harmony model for LS	-0.047	0.030	-0.034	0.042	S_4	S_4
f_{29}	average deviation from the best two color harmony models for LS	-0.055	0.037	-0.049	0.053	S_4	S_4
f_{30}	average lightness in LS	0.027	0.075	0.065	0.096	S_{11}	S_{11}
f_{31}	standard deviation of average lightness among the segments	0.080	0.076	-0.049	0.091	S_{15}	S_{15}
f_{32}	contrast of average lightness among the segments	0.075	0.067	-0.027	0.081	S_{15}	S_{15}
f_{33}	background size in Saliency Map (SM)	-0.165	0.082	-0.175	0.106	S_{16}	S_{16}
f_{34}	number of connected components in SM	-0.111	0.029	-0.062	0.088	S_{17}	S_{17}
f_{35}	size of the largest connected components in SM	0.132	0.075	0.036	0.073	S_{16}	S_{18}
f_{36}	average saliency weight of largest connected component	0.165	0.075	0.071	0.080	S_{16}	S_{18}
f_{37}	number of connected components in image background SM	-0.012	0.015	-0.035	0.038	S_{18}	S_{19}
f_{38}	size of the largest connected component of background in SM	-0.163	0.091	-0.145	0.052	S_{16}	S_{16}
f_{39}	distance between connected components in SM	0.117	0.056	-0.027	0.072	S_{17}	S_{17}
f_{40}	distance from rule of third points in SM	0.126	0.063	0.010	0.086	S_{17}	S_{17}
f_{41}	distance from center of image in SM	0.091	0.065	0.011	0.087	S_{17}	S_{17}
f_{42}	number of characters (OCR)	-0.082	0.057	-0.017	0.071	S_{19}	S_{20}
f_{43}	number of faces in the image	-0.035	0.008	-0.024	0.011	S_{20}	S_{21}

- [5] Cohen-Or, D., Sorkine, O., Gal, R., Leyvand, T., and Xu, Y.-Q. (2006). Color harmonization. In *ACM Transactions on Graphics*, pages 624–630.
- [6] Damera-venkata, N., Member, S., Kite, T. D., Geisler, W. S., Evans, B. L., Member, S., and Bovik, A. C. (2000). Image quality assessment based on a degradation model. *IEEE Trans. Image Processing*, pages 636–650.
- [7] Datta, R., Joshi, D., Li, J., and Wang, J. Z. (2006). Studying aesthetics in photographic images using a computational approach. In *ECCV*, pages 7–13.
- [8] Donthu, N., Lohtia, R., Osmonbekov, T., and Xie, T. (2004). Emotional appeal and incentive offering in banner advertisements. *Journal of Interactive Advertising*, pages 30–37.
- [9] Goldfarb, A. and Tucker, C. (2010). Online display advertising: Targeting and obtrusiveness. *Marketing Science*.
- [10] Gooch, B., Reinhard, E., Moulding, C., and Shirley, P. (2001). Artistic composition for image creation. In *Proceedings of the 12th Eurographics Workshop on Rendering Techniques*, pages 83–88.
- [11] Grant, M. and Boyd, S. (2011). CVX: Matlab software for disciplined convex programming, version 1.21.
- [12] Hou, X. and Zhang, L. (2007). Saliency detection: A spectral residual approach. *IEEE Computer Society Conference on Computer Vision and Pattern Recognition*, pages 1–8.
- [13] Isola, P., Xiao, J., Torralba, A., and Oliva, A. (2011). What makes an image memorable? In *IEEE Conference on Computer Vision and Pattern Recognition*, pages 145–152.
- [14] Itti, L., Koch, C., and Niebur, E. (1998). A model of saliency-based visual attention for rapid scene analysis. *IEEE Transactions on Pattern Analysis and Machine Intelligence*, pages 1254–1259.
- [15] Ke, Y., Tang, X., and Jing, F. (2006). The design of high-level features for photo quality assessment. In *CVPR*, pages 419–426.
- [16] Krishna, S. (2008). Open cv viola-jones face detection.
- [17] Li, C. and Chen, T. (2009). Aesthetic visual quality assessment of paintings. *IEEE Journal of Selected Topics in Signal Processing*, pages 236–252.
- [18] Li, H. and Bukovac, J. L. (1999). Cognitive impact of banner ad characteristics: An experimental study. *Journalism and Mass Communication Quarterly*, pages 341–53.
- [19] Luo, Y. and Tang, X. (2008). Photo and video quality evaluation: Focusing on the subject. In *ECCV*, pages 386–399.
- [20] McQuarrie, E. and Mick, D. (1999). Visual rhetoric in advertising: text-interpretive, experimental, and reader-response analyses. *Journal of consumer research*, pages 37–54.
- [21] Murtagh, F. (1983). A survey of recent advances in hierarchical clustering algorithms. *The Computer Journal*, pages 354–359.
- [22] Orlando, D. (2007). Optical character recognition.
- [23] Pass, G., Zabih, R., and Miller, J. (1996). Comparing images using color coherence vectors. In *Fourth ACM international conference on Multimedia*, pages 65–73.
- [24] Renjie, L. L., Lior, C., Cohen-or, W. D., Liu, L., Chen, R., Wolf, L., and Cohen-or, D. (2010). Optimizing photo composition. In *Computer Graphics Forum*, pages 469–478.
- [25] Richardson, M. (2007). Predicting clicks: Estimating the click-through rate for new ads. In *WWW*, pages 521–530.
- [26] Shi, J. and Malik, J. (2000). Normalized cuts and image segmentation. *IEEE Trans. Pattern Analysis and Machine Intelligence*, pages 888–905.
- [27] Tibshirani, R. (1996). Regression shrinkage and selection via the lasso. *Journal of the Royal Statistical Society*, pages 267–288.

- [28] Tokumaru, M., Muranaka, N., and Imanishi, S. (2002). Color design support system considering color harmony. In *Fuzzy Systems, 2002*, pages 378–383.
- [29] Tong, H., Li, M., jiang Zhang, H., He, J., and Zhang, C. (2004). Classification of digital photos taken by photographers or home users. In *Proceedings of Pacific Rim Conference on Multimedia*, pages 198–205.
- [30] Yaveroglu, I. and Donthu, N. (2008). Advertising repetition and placement issues in on-line environments. *Journal of Advertising*, pages 31–44.
- [31] Y.Mastuda (1995). Color design. In *Asakura Shoten*.